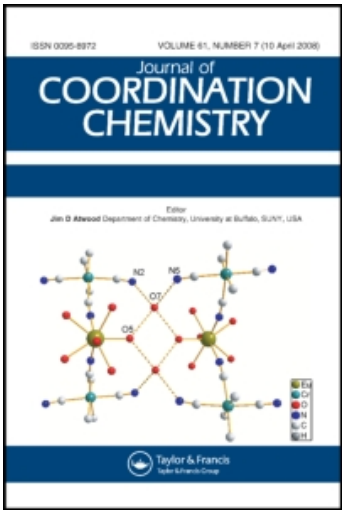

Journal of Coordination Chemistry
Publication details, including instructions for authors and subscription information:
http://www.informaworld.com/smpp/title~content=t713455674

Hydrothermal syntheses and structural characterization of two organic-inorganic hybrid compounds based on Lindqvist polyanions

Pengtao Ma[a]; Chunfa Yu[a]; Junwei Zhao[a]; Yuquan Feng[a]; Jingping Wang[a]; Jingyang Niu[a]
[a] Institute of Molecular and Crystal Engineering, School of Chemistry and Chemical Engineering, Henan University, Kaifeng, Henan 475001, P. R. China

To cite this Article Ma, Pengtao , Yu, Chunfa , Zhao, Junwei , Feng, Yuquan , Wang, Jingping and Niu, Jingyang(2009) 'Hydrothermal syntheses and structural characterization of two organic-inorganic hybrid compounds based on Lindqvist polyanions', Journal of Coordination Chemistry, 62: 19, 3117 — 3125
To link to this Article: DOI: 10.1080/00958970903030761
URL: http://dx.doi.org/10.1080/00958970903030761

Journal of Coordination Chemistry
Vol. 62, No. 19, 10 October 2009, 3117–3125

Taylor & Francis
Taylor & Francis Group

Hydrothermal syntheses and structural characterization of two organic–inorganic hybrid compounds based on Lindqvist polyanions

PENGTAO MA, CHUNFA YU, JUNWEI ZHAO, YUQUAN FENG, JINGPING WANG* and JINGYANG NIU*

Institute of Molecular and Crystal Engineering, School of Chemistry and Chemical Engineering, Henan University, Kaifeng, Henan 475001, P. R. China

(*Received 12 January 2009; in final form 19 March 2009*)

Two organic–inorganic hybrid polyoxometalates $\{[V_2W_4O_{19}\{Cu(2,2'\text{-bipy})_2\}_2]\cdot(4,4'\text{-bipy})\}_n$ (**1**) and $[Co(2,2'\text{-bipy})_3][W_6O_{19}]\cdot H_2O$ (**2**) (2,2′-bipy = 2,2′-bipyridine, 4,4′-bipy = 4,4′-bipyridine), constructed by Lindqvist polyanions and transition metal coordination cations, have been synthesized under hydrothermal conditions and characterized by elemental analysis, IR, UV spectra, thermogravimetric (TG) analyses, X-ray photoelectron spectroscopy (XPS), and single-crystal X-ray diffraction. Compound **1** is a neutral molecule and consists of a di-V^V substituted Lindqvist-type polyanion $[V_2W_4O_{19}]^{4-}$, two supporting copper cations $[Cu(2,2'\text{-bipy})_2]^{2+}$ and one free 4,4′-bipy. Neutral molecules of **1** are extended to a 2-D grid-like network by π–π stacking interactions between pyridine groups. The molecular structure of **2** contains one $[W_6O_{19}]^{2-}$ cluster polyanion and a $[Co(2,2'\text{-bipy})_3]^{2+}$. Inductively coupled plasma (ICP) analysis and XPS spectrum of **1** prove the presence of V^V. TG curves of **1** and **2** indicate two weight loss steps.

Keywords: Hydrothermal synthesis; Lindqvist anion; Polyoxometalates; Crystal structure

1. Introduction

The fabrication of organic–inorganic hybrid compounds is still very active due to the possibility of combining different characteristics of the components to obtain unusual structures, properties, or applications [1–3]. Polyoxometalates (POMs) composed of transition metals (W, Mo, V, Nb, and Ta) have been used as important molecular building blocks to construct inorganic–organic hybrid materials [4, 5]. In recent years, a large number of POM-based hybrids with various transition metal complexes have been reported [6–9] in which the transition metal coordination complexes function as charge compensation cations and/or become part of the inorganic POM framework. However, reports on organic–inorganic hybrids containing $[W_6O_{19}]^{2-}$ and V-substituted Lindqvist-type $[V_xW_{(6-x)}O_{19}]^{n-}$ clusters remain relatively rare [2]. A few compounds based on $[W_6O_{19}]^{2-}$ and $[V_xW_{(6-x)}O_{19}]^{n-}$ polyanions $[CpFeCpCH_2N(CH_3)_3]_2(W_6O_{19})$,

*Corresponding authors. Email: jpwang@henu.edu.cn; jyniu@henu.edu.cn

Journal of Coordination Chemistry
ISSN 0095-8972 print/ISSN 1029-0389 online
DOI: 10.1080/00958970903030761

$Co_2(4,4'\text{-bipy})_6(W_6O_{19})_2$, $[Cu(phen)_3][W_6O_{19}]$, $[Au_{11}(PPh_3)_8Cl_2]_2[W_6O_{19}]$, $[C_{16}H_{36}N]_3[HV_2W_4O_{19}]$, and $[CH_6N_3]_4[V_2W_4O_{19}]$ have been synthesized and characterized [10–14]. Since formation conditions are critical, the exploitation of this kind of compound remains challenging. The hydrothermal synthetic technique in combination with organic components has been a powerful strategy for the construction of organic–inorganic hybrid POMs [15, 16]. Following this strategy, we have synthesized two organic–inorganic hybrid Lindqvist-type polyoxometalates $\{[V_2W_4O_{19}\{Cu(2,2'\text{-bipy})_2\}_2]\cdot(4,4'\text{-bipy})\}_n$ and $[Co(2,2'\text{-bipy})_3][W_6O_{19}]\cdot H_2O$ (2,2′-bipy = 2,2′-bipyridine, 4,4′-bipy = 4,4′-bipyridine), which are characterized by elemental analysis, IR, UV spectra, thermogravimetric (TG) analyses, X-ray photoelectron spectroscopy (XPS), and single-crystal X-ray diffraction.

2. Experimental

2.1. *Materials and physical measurements*

All chemicals were of reagent grade and used without purification. All syntheses were carried out in 30 mL Teflon-lined autoclaves under autogenous pressure. The reaction vessels were filled to 60% volume capacity.

C, H, and N elemental analyses were performed on a Perkin-Elmer 240C elemental analyzer. Infrared spectra were recorded on a Nicolet 170 SXFT-IR spectrometer using KBr pellets from 400 to 4000 cm^{-1}. The UV spectra were recorded with a U-4100 spectrometer (DMSO as solvent) from 400 to 220 nm. TG-DTA measurements were carried out on a Perkin-Elmer7 thermal analyzer in flowing N_2 between 25 and 800°C at a heating rate of 10°C min^{-1}. XPS analyses were performed on an AXIS ULTRA spectrometer with an Al Kα achromatic X-ray source.

2.2. *Preparation of $\{[V_2W_4O_{19}\{Cu(2,2'\text{-bipy})_2\}_2]\cdot(4,4'\text{-bipy})\}_n$ (1)*

Compound **1** was prepared from a mixture of $CuCl_2\cdot 6H_2O$ (0.085 g, 0.50 mmol), $Na_2WO_4\cdot 2H_2O$ (0.660 g, 2.00 mmol), NH_4VO_3 (0.058 g, 0.50 mmol), 2,2′-bipy (0.05 g, 0.32 mmol), 4,4′-bipy (0.02 g, 0.13 mmol), and H_2O (15 mL, 0.83 mol). The starting mixture was carefully adjusted to pH = 9.5 by addition of 1.0 mol L^{-1} HCl solution and then stirred for 30 min in air. The final solution was transferred into a 30 mL polytetrafluoroethylene-lined stainless steel reaction container and heated to 160°C for 4 days. After cooling to room temperature, dark green prisms were filtered off, washed with distilled water and dried in air. Yield: 53% based on tungsten. Anal. Calcd (found) for **1** (wt%): H: 1.95 (2.02); C: 29.28 (28.69); N: 6.84 (6.92).

2.3. *Preparation of $[Co(2,2'\text{-bipy})_3][W_6O_{19}]\cdot H_2O$ (2)*

A mixture of $CoCl_2\cdot 6H_2O$ (0.119 g, 0.50 mmol), $Na_2WO_4\cdot 2H_2O$ (0.660 g, 2.00 mmol), NH_4VO_3 (0.058 g, 0.50 mmol), 2,2′-bipy (0.05 g, 0.32 mmol), and H_2O (15 mL, 0.83 mol) was sealed in a 30 mL Teflon-lined autoclave, adjusted by 1.0 mol L^{-1}

HCl solution to pH 7.5 and heated for 4 days at 160°C. After cooling to room temperature, orange block crystals of **2** were obtained. The product was filtered, washed with distilled water and dried in air. Yield: 45% based on tungsten. Anal. Calcd (found) for **2** (wt%): H: 1.33 (1.42); C: 18.46 (18.13); N: 4.31 (4.52).

2.4. *X-ray structure determination*

X-ray diffraction data were collected on a Bruker APEX-II CCD diffractometer at 296(2) K using Mo-Kα radiation ($\lambda = 0.71073$ Å). Intensity data were corrected for Lorentz and polarization effects. The structures were determined and the heavy atoms were found by direct methods and refined by full-matrix least-squares using SHELXL-97 [17]. The remaining atoms were found after successive Fourier syntheses. In **1**, the W2/V1 and W3/V2 positions are simultaneously statistically occupied by V^V and W^{VI} elements with half occupancy for each, resulting in two V^V ions per Lindqvist cage on the charge balance and crystallographic considerations, not uncommon in POM chemistry [18]. All the hydrogens attached to carbon atoms were placed in idealized positions and refined with a riding model using default SHELXL parameters. Hydrogens attached to lattice water were not located. The crystal data and structure refinements of **1** and **2** are summarized in table 1. Selected bond lengths (Å) and angles (°) are listed in tables 2 and 3.

Table 1. Crystallographic data and structural refinements of **1** and **2**.

	1	**2**
Empirical formula	$C_{50}H_{40}Cu_2N_{10}O_{19}V_2W_4$	$C_{30}H_{26}CoN_6O_{20}W_6$
Formula weight	2049.28	1950.58
Temperature (K)	296(2)	296(2)
Wavelength (Å)	0.71073	0.71073
Crystal system, space group	Triclinic, $P\bar{1}$	Cubic, P_213
Unit cell dimensions (Å, °)		
a	10.6996(10)	15.7754(4)
b	11.0783(10)	15.7754(4)
c	12.6794(12)	15.7754(4)
α	72.608(2)	90
β	77.350(2)	90
γ	71.3450(10)	90
V (Å^3)	1346.2(2)	3925.92(17)
Z	1	4
Calculated density (Mg m^{-3})	2.528	3.300
Absorption coefficient (mm^{-1})	9.700	18.007
F(000)	962	3508
Theta range for data collection (°)	2.00–25.00	1.83–25.08
Limiting indices	$-12 \le h \le 10$ $-12 \le k \le 13$ $-15 \le l \le 12$	$-17 \le h \le 17$ $-18 \le k \le 16$ $-6 \le l \le 18$
Reflections collected/unique	6919/4690 ($R_{int} = 0.0208$)	9228/2287 ($R_{int} = 0.0369$)
Goodness-of-fit on F^2	1.083	1.046
Final R indices [$I > 2\sigma(I)$]	$R_1 = 0.0401$, $wR_2 = 0.0990$	$R_1 = 0.0341$, $wR_2 = 0.0808$
R indices (all data)	$R_1 = 0.0477$, $wR_2 = 0.1016$	$R_1 = 0.0386$, $wR_2 = 0.0829$
Largest differential peak and hole (e Å^{-3})	1.706 and –1.818	1.107 and –1.639

Table 2. Selected bond lengths (Å) and angles (°) for **1**.

W1–O1	1.707(6)	W2|V1–O2	1.643(6)
W1–O4	1.914(6)	W2|V1–O6	1.890(7)
W1–O5	1.927(6)	W2|V1–O7	1.891(6)
W1–O9^{i}	1.928(6)	W2|V1–O5	1.930(6)
W1–O7^{i}	1.934(6)	W2|V1–O8	1.981(6)
W1–O10	2.2946(4)	W2|V1–O10	2.3080(6)
W3|V2–O3	1.663(7)	W3|V2–O4	1.915(6)
W3|V2–O6^{i}	1.884(6)	W3|V2–O8	1.955(6)
W3|V2–O9	1.900(6)	W3|V2–O10	2.2921(6)
Cu1–N2′	1.974(7)	Cu1–N1′	2.092(8)
Cu1–N1	1.976(8)	Cu1–N2	2.095(8)
Cu1–O8	2.031(6)	O1–W1–O4	103.6(3)
O4–W1–O5	88.0(3)	O6–W2|V1–O8	154.2(3)
O4–W1–O9^{i}	153.9(3)	O2–W2|V1–O10	178.1(3)
O1–W1–O10	179.4(2)	O6–W2|V1–O10	77.64(18)
O4–W1–O10	76.93(18)	O2–W2|V1–O6	104.2(3)
O3–W3|V2–O9	103.6(3)	O6–W2|V1–O7	89.0(3)
O9–W3|V2–O10	77.55(19)	O9–W3|V2–O8	86.7(3)
O9–W3|V2–O4	154.5(3)	O3–W3|V2–O10	177.8(3)
N2′–Cu1–N1	172.8(3)	N2′–Cu1–N2	80.1(3)
N2′–Cu1–N1′	94.5(3)	N1–Cu1–N2	98.5(3)
N1–Cu1–N1′	79.3(3)	N1′–Cu1–N2	109.9(3)

Symmetry transformations used to generate equivalent atoms: (i) $-x, -y, -z$.

Table 3. Selected bond lengths (Å) and angles (°) for **2**.

W1–O1	1.707(9)	W2–O2	1.684(9)
W1–O5	1.913(9)	W2–O6	1.893(9)
W1–O3	1.915(8)	W2–O7	1.906(8)
W1–O6^{i}	1.930(9)	W2–O7^{i}	1.919(8)
W1–O3^{i}	1.946(8)	W2–O5	1.960(8)
W1–O4	2.323(8)	W2–O4	2.287(8)
Co1–N1	1.910(9)	Co1–N1′	1.939(10)
O1–W1–O5	102.5(4)	O2–W2–O6	102.4(4)
O5–W1–O3	86.9(4)	O6–W2–O7	88.4(4)
O3–W1–O6^{i}	152.8(3)	O7–W2–O5	155.0(3)
O1–W1–O4	177.8(4)	O2–W2–O4	178.5(4)
O5–W1–O4	77.2(3)	O6–W2–O4	77.2(3)
N1–Co1–N1′	82.5(4)		

Symmetry transformations used to generate equivalent atoms: (i) y, z, x.

3. Results and discussion

3.1. *Synthesis*

In a specific hydrothermal process, many factors affect the crystal growth and the structure of products including initial reactants, temperature, pH, filling volume, and reaction time [19]. The crystallization of **1** is highly sensitive to the pH and the starting materials. It is crucial that the pH be adjusted to 9.5 in the formation of **1**; when the pH is lower, the desired product cannot be obtained. NH_4VO_3 as the vanadium source plays an important role in the formation of **1**. When NH_4VO_3 was substituted by V_2O_5, an unidentified sage green powder was obtained. Moreover, NH_4VO_3 is necessary for

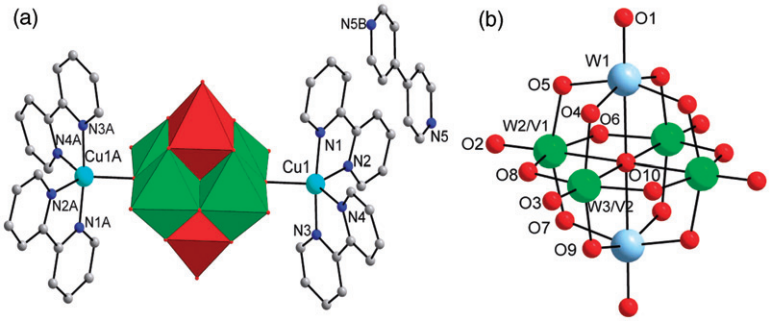

Figure 1. (a) The molecular structural unit of **1** with numbering scheme. The atoms with suffixes A and B are generated by the symmetrical operation: A: $-x$, $-y$, $-z$; B: $-x$, $1-y$, $1-z$. (b) The ball-and-stick representation of the di-V^V substituted polyanion $[V_2W_4O_{19}]^{4-}$.

formation of **2**, although **2** does not contain vanadium. When the reaction was performed in the absence of NH_4VO_3, nothing could be obtained except some yellow precipitate, which suggests that NH_4VO_3 can activate or induce the synthesis of **2**.

3.2. *Structural description*

Single crystal X-ray diffraction analysis reveals that the structural unit of **1** consists of one di-V^V substituted Lindqvist-type polyanion $[V_2W_4O_{19}]^{4-}$, two supporting copper-2,2′-bipy cations $[Cu(2,2'\text{-bipy})_2]^{2+}$, and one discrete 4,4′-bipy [figure 1(a)]. The di-V^V substituted Lindqvist-type polyanion $[V_2W_4O_{19}]^{4-}$ exhibits octahedral alignment constituted by six metal atoms [figure 1(b)]. Four metals (each metal site occupied by 1/2 V and 1/2 W) are arranged in a plane, bridged by a central oxygen (O10) and linked by four μ_2-O (O4, O9) to form an eight-membered ring. Two opposite sites of the plane are capped by tungstens [figure 1(b)]. According to the different coordination number, oxygens can be divided into four groups: 1 central μ_6-oxygen atom (O10), 6 terminal oxygens (O1, O2, O3), 10μ_2-oxygens (O4, O5, O6, O7, O9), and two μ_3-oxygens (O8). The (V/W)–O distances are between 1.643(6) and 2.3080(6) Å and W–O bond lengths vary from 1.707(6) to 2.2946(4) Å.

Two supporting copper-organic cations $[Cu(2,2'\text{-bipy})_2]^{2+}$ symmetrically link to $[V_2W_4O_{19}]^{4-}$ through two bridging oxygens [O(8)] with Cu–O distance of 2.031(6) Å. The five-coordinate Cu^{II} is a trigonal bipyramid, in which the equatorial plane is defined by two nitrogens from two 2,2′-bipy ligands [Cu–N: 1.976(8)–2.092(8) Å] and one oxygen from the Lindqvist-type polyanion $[V_2W_4O_{19}]^{4-}$ [Cu–O: 2.031(6) Å], and two nitrogens from two 2,2′-bipy ligands are axial [Cu–N: 1.974(7)–1.976(8) Å].

Close packing alignments in the solid-state via offset weak π–π interactions between neighboring pyridine rings of 2,2′-bipy along the *b*- and *c*-axis construct a 2-D, grid-like network. The inter-ring separation between adjacent pyridine rings is 4.32 Å along the *b*-axis and 4.15 Å along the *c*-axis, forming supramolecular rectangular nets with a size of *ca.* 8.25×9.05, encapsulating the 4,4′-bipyridine [20]. Face-to face π–π stacking interactions also exist between the aromatic rings of the 4,4′-bipyridine molecules and the aromatic rings of the neighboring 2,2′-bipyridine molecules with average distance of 3.8852 Å. Such π–π stacking interactions play a significant role in stabilization of the structure of **1**. The adjacent layers are in a close connection through weak van der

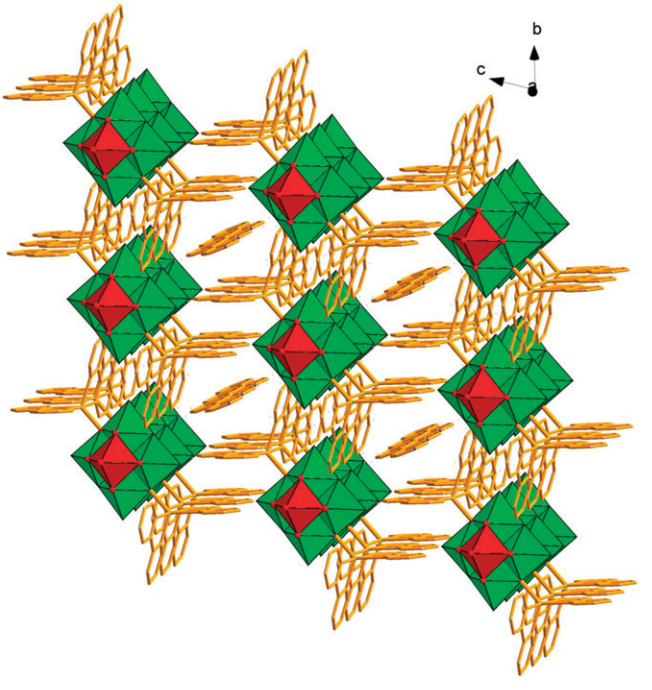

Figure 2. Packing diagram of **1** viewed down *a*-axis showing the grid-like cavity based on the neutral units $\{[V_2W_4O_{19}\{Cu(2,2'\text{-bipy})_2\}_2]\cdot(4,4'\text{-bipy})\}_n$ and encapsulated 4,4-bipy molecules.

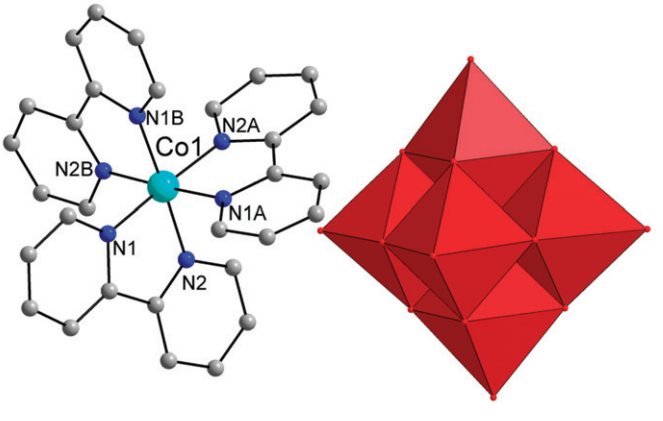

Figure 3. Molecular structure of **2**. The isolated water molecules and H atoms attached to 2,2′-bipy ligands are omitted for clarity. The atoms with suffixes A and B are generated by the symmetrical operation: A : $-1-z$, $0.5+x$, $-0.5-y$; B : $-0.5+y$, $-0.5-z$, $-1-x$.

Waals interaction, and the stacking motif is shown in figure 2. The porous compound may have application in catalysis and adsorption.

The molecular structure of **2** consists of three kinds of subunits: $[W_6O_{19}]^{2-}$ polyanion, $[Co(2,2'\text{-bipy})_3]^{2+}$ and one noncoordinating water. As shown in figure 3,

the polyanion of **2**, $[W_6O_{19}]^{2-}$, adopts the well-known super octahedral Lindqvist structure formed by six WO_6 octahedra connected with each other through edge-sharing oxygens and thus exhibits approximate O_h symmetry [12]. In this polyanion, W–O bond distances can be grouped into three sets according to the kind of oxygen bound to tungsten, W–O_t (terminal oxygen), 1.684(9)–1.707(9) Å, mean bond distance 1.696 Å; W–O_b (bridging oxygen), 1.893 (9)–1.960(8)Å, mean bond distance 1.920 Å; and W–O_c (central oxygen), 2.287(8)–2.323(8) Å, mean bond distance 2.305 Å. The geometric parameters are in agreement with those reported previously for related $[W_6O_{19}]^{2-}$ structures [12]. Besides $[W_6O_{19}]^{2-}$, there is a discrete cation $[Co(2,2'\text{-bipy})_3]^{2+}$ in a distorted CoN_6 octahedron with Co–N bond lengths in the range 1.910(9)–1.939(10) Å (av. 1.924 Å). Dihedral angles among the three ideal 2,2′-bipyridine planes in $[Co(2,2'\text{-bipy})_3]^{2+}$ are 82.97, 83.09, and 83.11°, indicating that the three ideal planes in $[Co(2,2'\text{-bipy})_3]^{2+}$ are not vertical to each other. This may be affected by the hexatungstate anions, verifying weak interactions between polyanions $[W_6O_{19}]^{2-}$ and $[Co(2,2'\text{-bipy})_3]^{2+}$ units.

3.3. *IR, UV, and XPS spectra*

The IR spectrum of **1** exhibits strong absorption peaks at 966, 955, 942, 800, and 772 cm^{-1}, attributed to ν(M=O) and ν(M–O–M) (M = W or V) bonds. The bridging M–O–M asymmetric stretching frequency has been split into two components (800 and 772 cm^{-1}) compared with that (781 cm^{-1}) of $K_4V_2W_4O_{19} \cdot 8H_2O$ [21], which may originate from Cu^{2+} cations bridging the di-V^V substituted Lindqvist-type polyanion $[V_2W_4O_{19}]^{4-}$; the remaining five bands are consistent with the IR spectrum of $K_4V_2W_4O_{19} \cdot 8H_2O$ [21]. Vibrations at 1599, 1582, 1532, 1496, 1443, 1400, 1319, 1175, 1031, and 1015 cm^{-1} are assigned to characteristic peaks of 2,2′-bipyridine and 4,4′-bipyridine. The IR spectrum of **2** exhibits prominent bands at 946 and 800 cm^{-1}, attributed to ν(W–O_t) and ν(W–O_b–W) bonds, respectively. Comparing the IR spectrum of **2** with that of $(TBA)_2[W_6O_{19}]$ [12], the peak of the W–O_t bond shifts from 978 to 947 cm^{-1}; ν(W–O_b–W) shifts from 815 to 800 cm^{-1}, which indicates that the $[W_6O_{19}]^{2-}$ polyoxoanion is affected by $[Co(2,2'\text{-bipy})_3]^{2+}$. In addition, intense bands at 1608, 1448, 1320, 1247, 1111, 1076, and 1041 cm^{-1} are assigned to 2,2′-bipyridine groups. The peak at 3450 cm^{-1} is assigned to water. Comparing the IR spectrum of **1** with that of **2**, obviously, the splitting absorption bands of ν(M=O) and ν(M–O–M) (M = W or V) bonds in **1** is related to V^V substituted for W^{VI} in $[V_2W_4O_{19}]^{4-}$.

The UV absorption spectrum of **1** exhibits an intense absorption at 251 nm (figure 4(a)), attributed to charge transitions of oxygens to metals (W and V) [21]. The UV absorption spectrum of **2** also reveals a strong absorption at 270 nm (figure 4(b)), assigned to charge transitions of $O \rightarrow W$ in the hexatungstate [12].

The XPS spectra of **1** in the energy regions of Cu_{2p}, V_{2p}, and W_{3d} show peaks at 934.10, 516.7, and 35.1 eV, attributable to Cu^{2+}, V^{5+}, and W^{6+}, respectively (figure 5). These results are consistent with the binding energy values of Cu_{2p} in CuO [22], V_{2p} in V_2O_5 [23], and W_{3d} in α-$SiW_{12}O_{40}$ [24], which are 934.1, 516.6, and 35.3 eV, respectively. These observations are in agreement with the results of the single-crystal X-ray analysis.

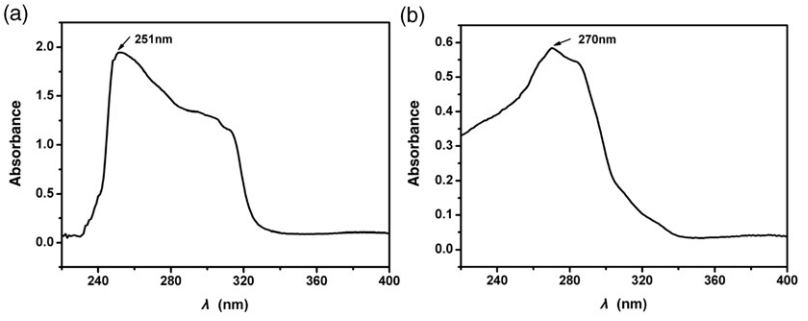

Figure 4. The UV absorption spectra of (a) **1** and (b) **2**.

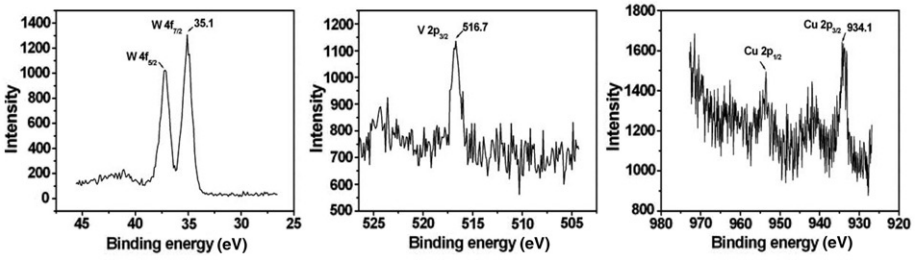

Figure 5. XPS spectra of **1**.

3.4. *Thermogravimetric (TG) analysis*

The TG curve of **1** has two weight loss steps (Supplementary Material). The first weight loss of 7.90% from 25 to 400°C corresponds to loss of free 4,4′-bipyridine (Calcd 7.62%). The second weight loss of 30.15% between 400 and 610°C is attributed to decomposition of four 2,2′-bipyridine ligands, in agreement with the calculated value (30.49%). The TG curve of **2** also exhibits two weight loss steps. The first is 1.31% in the temperature range 25–120°C, corresponding to the release of water. The second weight loss is 22.56% from 200 to 550°C, assigned to the release of 2,2′-bipyridine groups. The whole weight loss (23.87%) is consistent with the calculated value (24.92%).

4. Conclusions

Two organic–inorganic hybrid polyoxometalates $\{[V_2W_4O_{19}\{Cu(2,2'\text{-bipy})_2\}_2] \cdot (4,4'\text{-bipy})\}_n$ (**1**) and $[Co(2,2'\text{-bipy})_3][W_6O_{19}] \cdot H_2O$ (**2**) are constructed by Lindqvist polyanions and transition metal coordination cations, and characterized by elemental analysis, IR, UV spectra, TG analyses, XPS spectra, and single-crystal X-ray diffraction. The synthesis and isolation of **1** and **2** provide useful information for exploring other Lindqvist-type polyoxometalates by the hydrothermal method.

Supplementary material

Crystallographic data for the structural analysis reported in this article have been deposited with the Cambridge Crystallographic Data Centre with the deposited CCDC numbers 715137, 715138 for **1** and **2**. Copies of this information may be obtained free of charge from The Director, CCDC, 12 Union Road, Cambridge, CB2 1EZ, UK (Fax: +44-1223-336033; E-mail: deposit@ccdc.cam.ac.uk).

Acknowledgements

This work was financially supported by the National Natural Science Foundation of China, Program for New Century Excellent Talents in University of Henan Province, the Foundation of Education Department of Henan Province, and the Natural Science Foundation of Henan Province.

References

[1] J.Y. Niu, Q.X. Han, J.P. Wang. *J. Coord. Chem.*, **56**, 523 (2003).
[2] P.J. Hagraman, D. Hagraman, J. Zubieta. *Angew. Chem. Int. Ed. Engl.*, **38**, 2638 (1999).
[3] F. Hussain, U. Kortz, B. Keita, L. Nadjo, M.T. Pope. *Inorg. Chem.*, **45**, 761 (2006).
[4] U. Kortz, M.G. Savelieff, F.Y. Abou-Ghali, L.M. Khalil, S.A. Maalouf, D.I. Sinno. *Angew. Chem. Int. Ed. Engl.*, **41**, 4070 (2002).
[5] X. Huang, J. Li, H. Fu. *J. Am. Chem. Soc.*, **122**, 8789 (2000).
[6] J.Y. Niu, Z.L. Wang, J.P. Wang. *J. Coord. Chem.*, **57**, 411 (2004).
[7] X.L. Wang, H.Y. Lin, Y.F. Bi, B.K. Chen, G.C. Liu. *J. Solid State Chem.*, **181**, 556 (2008).
[8] J.Q. Sha, C. Wang, J. Peng, J. Chen, A.X. Tian, P.P. Zhang. *Inorg. Chem. Commun.*, **10**, 321 (2007).
[9] Z.M. Zhang, S. Yao, E.B. Wang, C. Qin, Y.F. Qi, Y.G. Li, R. Clerac. *J. Solid State Chem.*, **181**, 715 (2008).
[10] P.L. Veya, J.K. Kochi. *J. Organomet. Chem.*, **488**, C4 (1995).
[11] L.J. Zhang, Y.G. Wei, C.C. Wang, H.Y. Guo, P. Wang. *J. Solid State Chem.*, **177**, 3433 (2004).
[12] F.X. Meng, K. Liu, Y.G. Chen. *Chinese J. Struct. Chem.*, **25**, 837 (2006).
[13] M. Schulz-Dobrick, M. Jansen. *Z. Anorg. Allg. Chem.*, **633**, 2326 (2007).
[14] C.J. Besecker, V.W. Day, W.G. Klemperer, M.R. Thompson. *J. Am. Chem. Soc.*, **125**, 5928 (2003).
[15] (a) B.Z. Lin, S.X. Liu. *Polyhedron*, **19**, 2521 (2000); (b) L.M. Zheng, Y. Wang, X. Wang, J.D. Korp, A.J. Jacobson. *Inorg. Chem.*, **40**, 1380 (2001); (c) R.C. Finn, J. Sims, C.J. O'Connor, J. Zubieta. *J. Chem. Soc., Dalton Trans.*, 159 (2002).
[16] (a) A.M. Chippindale, A.D. Law. *J. Solid State Chem.*, **142**, 236 (1999); (b) Z. Shi, S.H. Feng, S. Gao, L.R. Zhang, G.Y. Yang, J. Hua. *Angew. Chem. Int. Ed.*, **39**, 2325 (2000); (c) S.X. Liu, B.Z. Lin, S. Lin. *Inorg. Chim. Acta*, **304**, 33 (2000).
[17] G.M. Sheldrick. SHEXTL-97, Programs for Crystal Structure Refinement, University of Göttingen, Germany (1997).
[18] S. Reinoso, P. Vitoria, L.S. Felices, L. Lezama, J.M. Gutiérrez-Zorrilla. *Chem. Eur. J.*, **11**, 1538 (2005).
[19] (a) K. Pavani, A. Ramanan. *Eur. J. Inorg. Chem.*, 3080 (2007); (b) K. Pavani, S.E. Lofland, K.V. Ramanujachary, A. Ramanan. *Eur. J. Inorg. Chem.*, 568 (2005).
[20] J.P. Wang, G.Q. Zhang, P.T. Ma, J.Y. Niu. *Inorg. Chem. Commun.*, **11**, 825 (2008).
[21] C.M. Flynn, M.T. Pope. *Inorg. Chem.*, **10**, 2524 (1971).
[22] V.I. Nefedov, M.N. Firsov, I.S. Shaplygin. *J. Electron Spectrosc. Relat. Phenom.*, **26**, 65 (1982).
[23] (a) R. Larsson, B. Folkesson, G. Schön. *Chem. Scr.*, **3**, 88 (1973); (b) J. Kasperkiewicz, J.A. Kovacich, D.J. Lichtman. *J. Electron Spectrosc. Relat. Phenom.*, **32**, 128 (1983).
[24] Y.H. Feng, Z.G. Han, J. Peng, J. Lu, B. Xue, L. Li, H.Y. Ma, E.B. Wang. *Mater. Lett.*, **60**, 1588 (2006).